

Formation of the Early Photoproduct Lumi-R of Cyanobacterial Phytochrome Cph1 Observed by Ultrafast Mid-Infrared Spectroscopy

Jasper J. van Thor,^{*,†} Kate L. Ronayne,[‡] and Michael Towrie[‡]

Contribution from the Laboratory of Molecular Biophysics, University of Oxford, Rex Richards Building, South Parks Road, Oxford OX1 3QU, U.K., and Central Laser Facility, CCLRC Rutherford Appleton Laboratory, Chilton, Didcot, Oxfordshire, OX11 0QX, U.K.

Received August 21, 2006; E-mail: jasper@biop.ox.ac.uk

Abstract: The photoreactions of the Pr ground state of cyanobacterial phytochrome Cph1 from *Synechocystis* PCC 6803 have been investigated by picosecond time-resolved mid-infrared spectroscopy at ambient temperature. With femtosecond excitation of the Pr state at 640 nm, the photoisomerized Lumi-R product state is generated with kinetics and associated difference spectra indicative of vibrational cooling with $\tau_1 = 3$ ps time constant and excited state decay with $\tau_1 = 3$ ps, $\tau_2 = 14$ ps, and $\tau_3 = 134$ ps time constants. The Lumi-R state is characterized by downshifted absorption of three C=C modes assigned to C₁₅=C₁₆, C₄=C₅, and a delocalized C=C mode, in addition to the downshifted C₁₉=O mode. The Lumi-R minus Pr difference spectrum is indicative of global restructuring of the chromophore on the ultrafast timescale, which is discussed in light of C₁₅ Z/E photoisomerization in addition to changes near C₅, which could be low bond order torsional angle changes.

Introduction

Phytochromes are red and far-red light receptors that contain signaling kinase domains and have been found and characterized in plants, bacteria, and cyanobacteria, where they play various physiological roles.^{1–4} It is widely accepted that photoreception by phytochromes is triggered by photoisomerization reactions as in the opsin receptors, but fundamental questions remain regarding the nature of photochemical and thermal reactions and the chromophore structure in the “Pfr” photoproduct and intermediates.^{5,6} The spectroscopic transitions of *Synechocystis* Cph1 are similar to those observed in plant phytochrome receptors, distinguishing the red light absorbing (~650 nm) “Pr” ground state and far-red light absorbing (~710 nm) “Pfr” metastable intermediate that can be reversibly phototransformed.^{7,8} One important biological aspect is the low quantum yield of phototransformation of phytochromes,^{4,8–10} which is yet to be

understood in terms of the initial photoreactions and barriers in the phototransformation pathway. Specifically, solid evidence for C₁₅ Z/E photoisomerization and several resulting thermal reactions in the phototransformation pathway has not yet been provided. The X-ray structure of a fragment of the *Deinococcus radiodurans* bacterial phytochrome DrBph in the Pr state was recently reported, which provided evidence for a C₄-Z, C₁₀-Z, C₁₅-Z, C₅-syn, C₁₀-syn, C₁₅-anti (ZZZssa; Scheme 1) conformation of the biliverdin chromophore and the steric possibility for C₁₅ Z/E photoisomerization.⁵ The ZZZssa conformation was also determined for the phycocyanobilin chromophore in a proteolytic fragment of Cph1 by NMR spectroscopy.⁶ Further evidence supporting C₁₅ Z/E photoisomerization is that mutation of Y176 in *Synechocystis* Cph1 abolished phototransformation of Pr,¹¹ which is a conserved residue found to contact the D-ring in the *D. radiodurans* Bph.⁵

Experimental evidence suggests, however, that the phototransformation is likely to be more complex. First, the Lumi-R product formed on a picosecond timescale is red-shifted only a few nanometers relative to the Pr ground state absorption,¹² and the major red-shifted products are formed thermally only on microsecond and millisecond timescales.^{7,8} C₁₅ Z/E isomerization is predicted to red-shift the optical absorption,⁶ and the nature of the several thermal reactions is unknown. Second, details from a reaction model based on resonance Raman spectroscopy and normal mode calculations predicted a partial C₅–C₆ anti to syn bond rotation in addition to a C₁₅ Z/E photoisomerization in

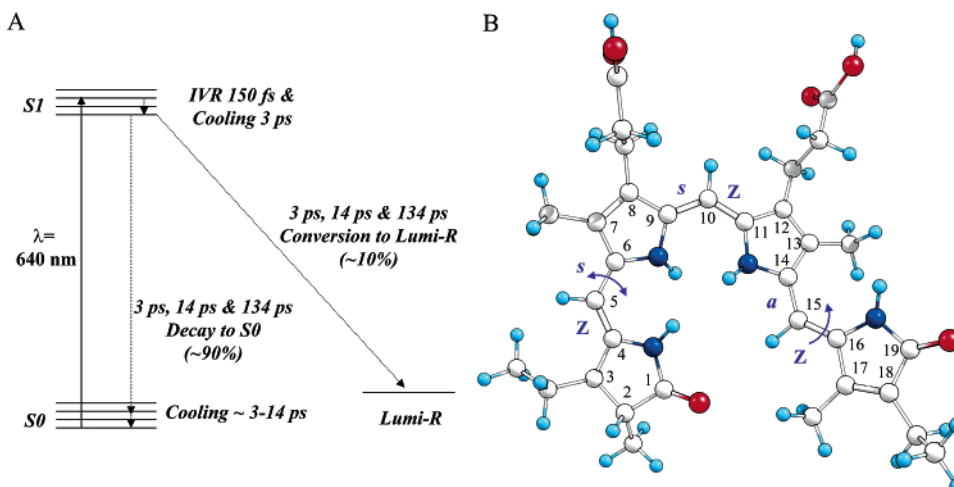
[†] University of Oxford.

[‡] CCLRC Rutherford Appleton Laboratory.

- (1) Montgomery, B. L.; Lagarias, J. C. *Trends Plant Sci.* **2002**, *7*, 357.
- (2) Lamparter, T. *FEBS Lett.* **2004**, *573*, 1.
- (3) Yeh, K. C.; Wu, S. H.; Murphy, J. T.; Lagarias, J. C. *Science* **1997**, *277*, 1505.
- (4) Butler, W. L.; Norris, K. H.; Siegelman, H. W.; Hendricks, S. B. *Proc. Natl. Acad. Sci. U.S.A.* **1959**, *45*, 1703.
- (5) Wagner, J. R.; Brunzelle, J. S.; Forest, K. T.; Vierstra, R. D. *Nature* **2005**, *438*, 325.
- (6) van Thor, J. J.; Mackeen, M.; Kuprov, I.; Dwek, R. A.; Wormald, M. R. *Biophys. J.* **2006**, *91*, 1811.
- (7) Remberg, A.; Lindner, I.; Lamparter, T.; Hughes, J.; Kneip, C.; Hildebrandt, P.; Braslavsky, S. E.; Gartner, W.; Schaffner, K. *Biochemistry* **1997**, *36*, 13389.
- (8) van Thor, J. J.; Borucki, B.; Crielgaard, W.; Otto, H.; Lamparter, T.; Hughes, J.; Hellingwerf, K. J.; Heyn, M. P. *Biochemistry* **2001**, *40*, 11460.
- (9) Gensch, T.; Churio, M.; Braslavsky, S.; Schaffner, K. *Photochem. Photobiol.* **1996**, *63*, 719.
- (10) Kelly, J. M.; Lagarias, J. C. *Biochemistry* **1985**, *24*, 6003.

(11) Fischer, A. J.; Lagarias, J. C. *Proc. Natl. Acad. Sci. U.S.A.* **2004**, *101*, 17334.

(12) Heyne, K.; Herbst, J.; Stehlik, D.; Esteban, B.; Lamparter, T.; Hughes, J.; Diller, R. *Biophys. J.* **2002**, *82*, 1004.

Scheme 1 Proposed Reaction Scheme for the Photoreactions and Time Constants of the Pr State of Cph1 (A) and Phycocyanobilin Chromophore of Cyanobacterial Cph1 in the ZZZssa Conformation (B)^a

^a Bond conformations are indicated with Z, s, and a labels. Carbon atoms are numbered following the convention for tetrapyrroles, and arrows indicate thermal C₅-C₆ torsional motion and C₁₅=C₁₆ Z/E photoisomerisation, respectively.

the Pr to Pfr pathway.^{13,14} Finally, recent ¹³C NMR measurements on isotopically labeled chromophore in *Synechocystis* Cph1 showed reversible light-induced changes of the resonance frequency of C₄, which could be explained by either photoisomerization at C₄ or by thermal C₅-C₆ bond rotation in addition to C₁₅ Z/E isomerization.⁶ Assignments of infrared active modes from static FTIR measurements of the photoreactions of phytochromes have been addressed and developed experimentally using model compound studies and isotopic substitution strategies.¹⁵⁻¹⁸ Here, we have used ultrafast mid-infrared pump-probe spectroscopy¹⁹⁻²² and present the vibrational response of the chromophore on an ultrafast timescale after photoisomerization and restructuring of the Pr ground state.

Experimental Section

Time-Resolved Mid-Infrared Spectroscopy. The holoform of the 58 kDa N-terminal fragment of *Synechocystis* PCC 6803 Cph1 was coexpressed together with the *hemA* heme oxygenase and *pcyA* bilin reductase genes from *Synechocystis*, as described previously.¹⁸ The sample was concentrated to 0.9 mM in D₂O with 5 mM Tris/HCl pD 7.8 and loaded into a closed circulating flow systems and was used at 291 K. A 5-mL volume was flowed continuously using a Harrick flow cell with a 50- μ m path length using CaF₂ windows, providing an OD_{655nm} of 0.4 and a maximum absorption of ~0.8 in the amide I region. Measurements were performed at the PIRATE ultrafast infrared absorption facility at the Rutherford Appleton Laboratory, Chilton.¹⁹ Briefly, the sample was excited with 640-nm, 150-fs pulses with 2 μ J

of energy at 0.5 kHz repetition rate and probed with ~150 cm⁻¹ fwhm broadband infrared pulses at 1 kHz. The spot size was 200 μ m and 150 μ m diameter for the pump and the probe beam, respectively. The difference signal pump-on minus pump-off was normalized on a shot-by-shot basis and typically accumulated for six successive rounds of 20-s data integration for a single time delay. The infrared beams were dispersed by 150 l/mm, 4000-nm blaze, gold grating monochromators and imaged onto 64 element MCT-13-64e photoconductive detectors. The data were collected in two 150 cm⁻¹ spectral windows centered at 1680 and 1540 cm⁻¹ using the delay line for optical delays between 2 ps and 2 ns, at 2, 3, 4, 5, 7, 10, 13, 17, 22, 27, 33, 39, 50, 60, 75, 100, 130, 200, 250, 300, 400, 500, 625, 750, 875, 1000, 1250, 1500, 1750, and 2000 ps. The difference signal was referenced using water lines present in the probe spectrum, and the two spectral windows were interleaved after scaling using overlapping transients recorded at the same delay time. The sample was raster scanned in *x*- and *y*- directions at an approximate rate of 100 μ m/ms and continuously illuminated with strong far-red background light to reform the Pr state, provided by a 250 W KL 2500 light source (Schott) delivered via an optical fiber and filtered by an RG9 710-nm high-pass filter (Schott). To test for potential accumulation of photoproduct, 30-s continuous pulsed laser excitation at 640 nm was combined with far-red light illumination, and the absorption was subsequently scanned, which showed only the Pr state present. Furthermore, the low quantum yield of formation of the Lumi-R state ensured that, together with raster scanning, transient absorption due to excitation of intermediates was not significant and contributed <10% to the signal. Additionally, the fitted time constants were very similar to those found from transient absorption measurements that have no possible contribution from excitation of intermediates.¹²

Computational Details. All calculations were performed with Gaussian 03.²³ For geometry optimization and normal mode calculation and calculation of infrared frequencies and intensities, a phycocyanobilin chromophore model was used on the basis of the coordinates of the biliverdin chromophore in the ZZZssa conformation (Scheme 1) in DrBph,⁵ with replacement of the propionate carboxylic acid groups with hydrogens. All four nitrogens were included as deuterated in the calculations. Density functional theory calculations reported in this study were performed at the DFT B3LYP 6-31G(d,p) level using increased optimization restraints and ultrafine grid parameters for the Hessian calculations on fully optimized geometries. Normal mode calculations of these geometries generated no imaginary frequencies.

- (13) Kneip, C.; Hildebrandt, P.; Schlamann, W.; Braslavsky, S. E.; Mark, F.; Schaffner, K. *Biochemistry* **1999**, *38*, 15185.
- (14) Mroginski, M. A.; Murgida, D. H.; von Stetten, D.; Kneip, C.; Mark, F.; Hildebrandt, P. *J. Am. Chem. Soc.* **2004**, *126*, 16734.
- (15) Siebert, F.; Grimm, R.; Rudiger, W.; Schmidt, G.; Scheer, H. *Eur. J. Biochem.* **1990**, *194*, 921.
- (16) Foerstendorf, H.; Benda, C.; Gartner, W.; Storf, M.; Scheer, H.; Siebert, F. *Biochemistry* **2001**, *40*, 14952.
- (17) Foerstendorf, H.; Lamparter, T.; Hughes, J.; Gartner, W.; Siebert, F. *Photochem. Photobiol.* **2000**, *71*, 655.
- (18) van Thor, J. J.; Fisher, N.; Rich, P. R. *J. Phys. Chem. B* **2005**, *109*, 20597.
- (19) Towrie, M.; Grills, D. C.; Dyer, J.; Weinstein, J. A.; Matousek, P.; Barton, R.; Bailey, P. D.; Subramaniam, N.; Kwok, W. M.; Ma, C.; Phillips, D.; Parker, A. W.; George, M. W. *Appl. Spectrosc.* **2003**, *57*, 367.
- (20) Hamm, P.; Ohline, S. M.; Zinth, W. *J. Chem. Phys.* **1996**, *106*, 519.
- (21) Groot, M. L.; van Wilderen, L. J.; Larsen, D. S.; van der Horst, M. A.; van Stokkum, I. H.; Hellingwerf, K. J.; van Grondelle, R. *Biochemistry* **2003**, *42*, 10054.
- (22) Heyne, K.; Mohammed, O. F.; Usman, A.; Dreyer, J.; Nibbering, E. T.; Cusanovich, M. A. *J. Am. Chem. Soc.* **2005**, *127*, 18100.

- (23) Frisch, M. J.; et al. *Gaussian 03*, revision D.01; Gaussian, Inc.: Wallingford, CT, 2004.

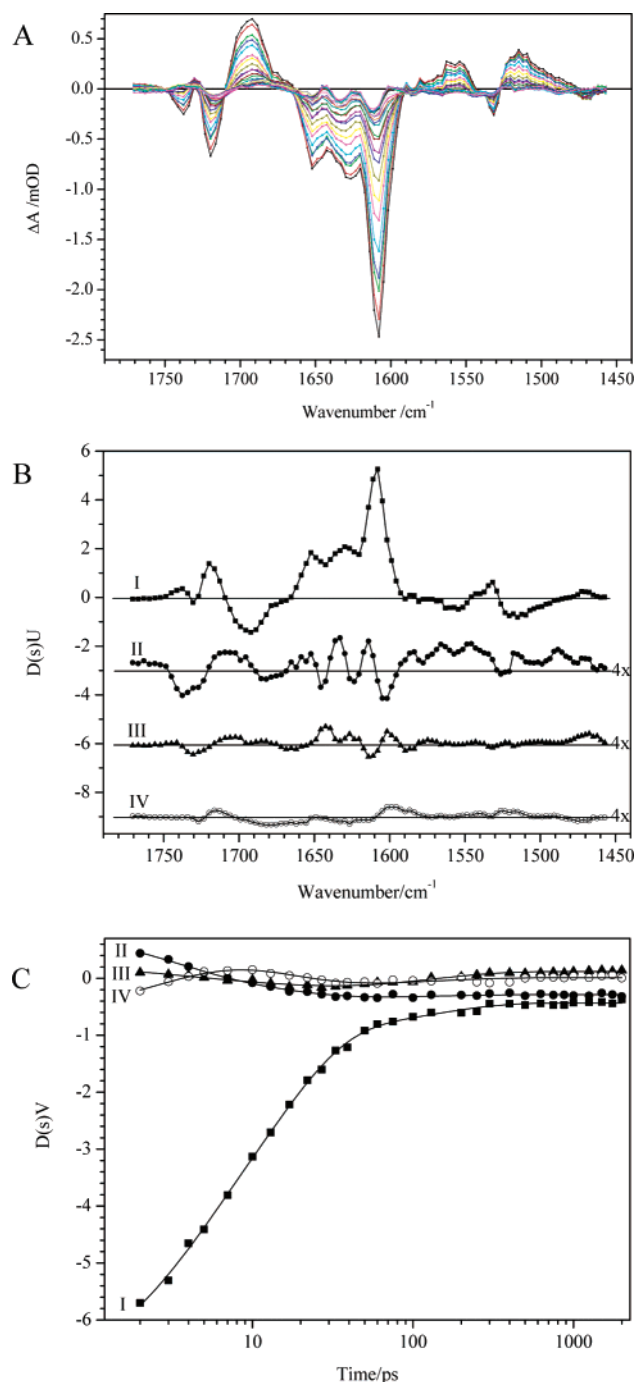


Figure 1. Transient mid-infrared absorption changes of Pr between 1750 and 1450 cm^{-1} . (A) Pump-on minus pump-off difference spectra at 30 delays between 2 ps and 2 ns (see Experimental Section). A negative time spectrum collected at -50 ps has been subtracted. (B) Singular value decomposition (SVD) analysis following $\Delta A = UD(s)V^T$ provided scaled $D(s)U$ basis spectra I (■), II (●), III (▲), and IV (○), which had singular values 0.01236, 0.00154, 0.00055, and 0.00042. (C) Corresponding scaled time traces $D(s)V^T(t)$, which were fitted with three time constants $\tau_1 = 3$ ps, $\tau_2 = 14$ ps, and $\tau_3 = 134$ ps.

Results and Discussion

Time-resolved mid-infrared absorption measurements of the Pr state with femtosecond visible excitation pulses at 640 nm using delays between 2 ps and 2 ns monitored the dominant excited state decay reactions (90%) and the formation with low yield (10%) of the early Lumi-R photoproduct (Scheme 1, Figure 1A). Measurements in the spectral region between 1750

and 1450 cm^{-1} covered the absorption changes of C=O and C=C modes that report on electronic decay, photoisomerization, and restructuring on an ultrafast timescale. At frequencies below 1450 cm^{-1} , difference features were of much reduced intensity, particularly of the Lumi-R product state that is formed with low quantum yield, as in the Pfr product state.¹⁸ Singular value decomposition of the transient infrared absorption data provided four relevant spectral components (Figure 1B). Fitting of the scaled time traces supported three time constants for the transient infrared absorption data up to 2 ns, $\tau_1 = 3$ ps (38%), $\tau_2 = 14$ ps (52%), and $\tau_3 = 134$ ps (10%) (Figure 1C), whereas fitting with only two time constants was unsatisfactory. The three time constants are additionally supported by visual inspection of fitted single wavelength traces, for example at 1734 and 1526 cm^{-1} , where sign changes of the amplitudes of the 14- and 134-ps components and the 3- and 14-ps components are evident, respectively (Figure 2). Thus, the data support a clear level of complexity of the decay and phototransformation reactions, which was further supported by independently repeated measurements and data fitting.

Figure 3 shows the corresponding globally fitted spectra of the three decay components (panel A). The spectra belonging to the 3- and 14-ps components are similar but have different positions of equivalent S1 and S0 modes; the 14-ps component has slightly higher frequency bands and the 134-ps component has lower frequency bands compared to the 3-ps component. The upshifted S1 modes in the 14 ps relative to those in the 3-ps component, for example at 1696 cm^{-1} , may be explained by vibrational cooling of the S1 state with a time constant similar to the 3-ps time constant fitted for the electronic decay pathway. The upshifted S0 bands in the 14 ps relative to those in the 3-ps spectrum may indicate formation of a thermally excited ground state on this timescale, resulting from the dominant excited state decay reactions. The frequency differences of S1 and S0 states in the 3- and 14-ps components may therefore be indicative of subsequent thermal cooling reactions where cooling is occurring on timescales that also match electronic decay kinetics. This interpretation relies on the generalized effect of the anharmonicity constants in Taylor's expansion of the molecular energy on the absorption and stimulated emission contributions to the line shape, on both S1 and S0 modes.²⁰ It is assumed that in S1 ultrafast, femtosecond timescale, intramolecular vibrational redistribution (IVR) occurs, which is supported by the observation in transient visible absorption of a relaxation reaction with a 150-fs time constant.¹² This global fit procedure therefore described the observed spectral changes, which have complex underlying dynamics, fitted with the minimum number of parameters.

The third decay pathway, at 134 ps, is considered to be too long for cooling processes and is assigned to a slow decay component of S1. The spectral differences with the fast components are taken as an indication of the presence of a population that has different S1 and S0 vibrational energies. This is interpreted as structurally heterogeneous populations of the phycocyanobilin chromophore in the Pr ground state, possibly through angle differences of the methine bridge bonds, that is resolved in this data as well as in other independent measurements. This would also be in accord with conclusions from NMR spectroscopy⁶ and fluorescence spectroscopy²⁴ as well as ultrafast visible absorption spectroscopy,¹² which

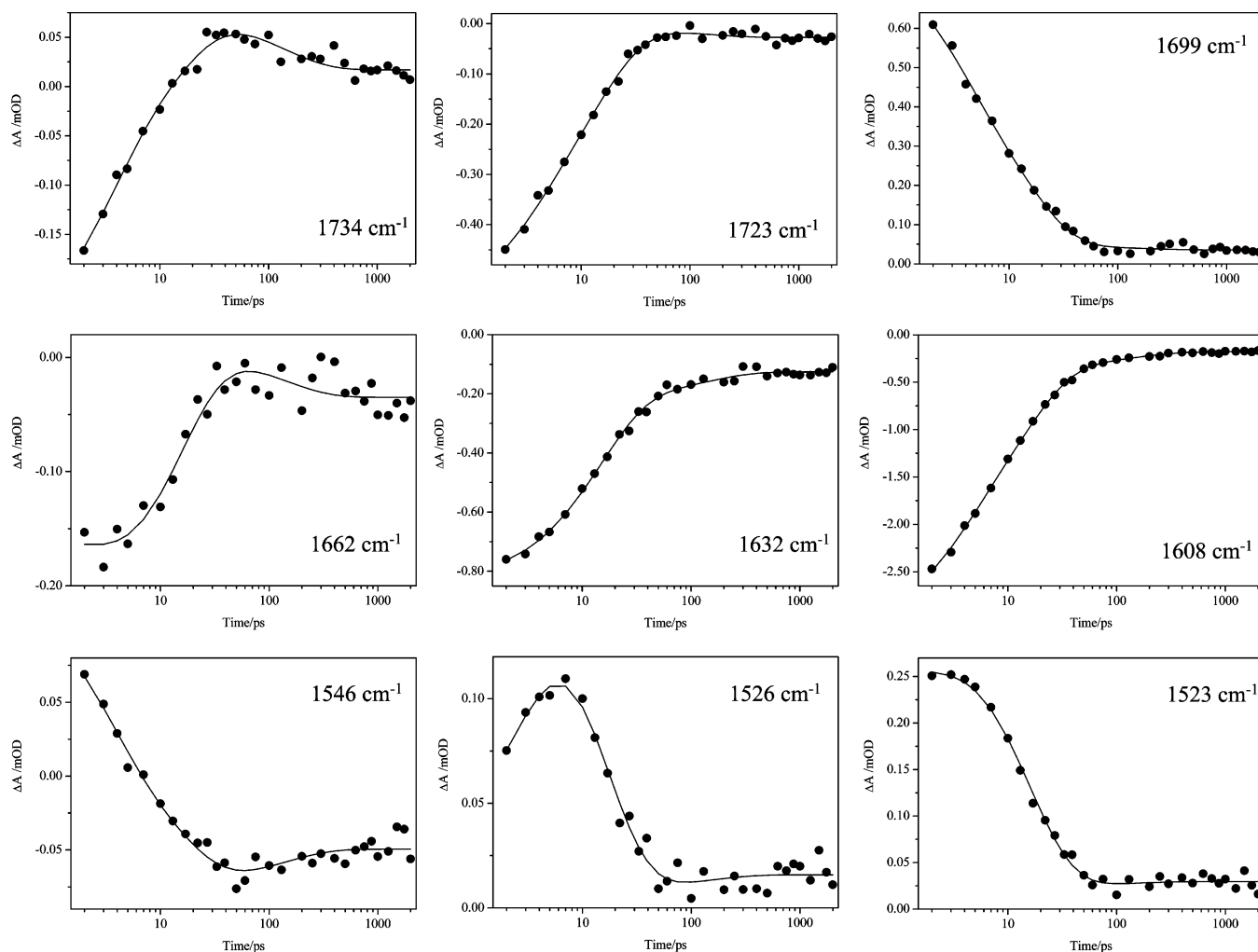


Figure 2. Global fitting of the transient difference absorption of Pr 9 out of 103 globally fitted traces using the time constants $\tau_1 = 3$ ps, $\tau_2 = 14$ ps, and $\tau_3 = 134$ ps obtained from SVD.

supported a distribution of electronic decay time constants that are in agreement with those assigned on the basis of transient infrared absorption (Figure 3A). The similarity of the associated spectrum with that of the early decay phases also supports this interpretation, whereas the possibility of rearrangements in S0 associated with the 134-ps phase prior to formation of Lumi-R would introduce a new intermediate for which no evidence has been put forward thus far.¹²

An early ground-state product “Lumi-R” is formed with a low amplitude, which corresponds to a low ($\sim 10\%$) quantum yield and is stable on the nanosecond timescale (Figure 3B). The measurements did not detect the relative quantum yield of each electronic decay phase for formation of the Lumi-R state, and equal yield was assumed for the fitting of their associated spectra, with the Lumi-R minus Pr difference spectrum determined by late time point measurements. Strikingly, the Lumi-R minus Pr difference spectrum resembles the short-lived decay spectra that are characterized by general downshifts via bond order reduction (Figure 3A), but since Lumi-R is not a singlet state the downshifts are the result of isomerization and restructuring. This also indicates that the Lumi-R minus Pr difference spectrum is dominated by chromophore modes, as

expected on the short timescale. The $C_1=O$ and $C_{19}=O$ modes are found at $\sim 1738(-)/1732(+)$ and $\sim 1720(-)/1692(+)$ cm^{-1} in the three decay spectra (Figure 3A), in agreement with previous assignments based on ^{13}C isotopic substitution¹⁸ and supported by DFT normal mode calculations (Figure 4; Table 1). In the Lumi-R minus Pr difference spectrum, the $C_1=O$ mode at 1738 cm^{-1} appears to have increased in cross section, whereas the $C_{19}=O$ mode is strongly downshifted $1716(-)/1685(+)$ cm^{-1} (Figure 3B).

This first time-resolved observation of the infrared absorption of this initial photoproduct is substantially different from a cryo-trapped photoproduct of Cph1, assigned to the meta-Ra intermediate rather than lumi-R¹⁷ and also from the cryo-trapped Lumi-R state of oat phytochrome.¹⁶ In particular, the downshift of the 1716 cm^{-1} mode to 1685 cm^{-1} , which is assigned to $C_{19}=O$,¹⁸ contrasts with the upshifted frequency observed in cryo-trapped intermediates in Cph1 and oat phytochrome.^{16,17} Considering that C_{15} Z/E isomerization could reduce H-bonding interactions to $C_{19}=O$, which in the DrBph structure directly interacts with His290,⁵ this might rationalize the upshift in the case of the cryo-trapped product but not the downshift observed in the primary photoproduct Lumi-R at ambient temperature from the time-resolved data (Figure 3B). It should be noted that in the case of Cph1 the first photoproduct of Pr was generated

(24) Sineshchekov, V.; Koppel, L.; Esteban, B.; Hughes, J.; Lamparter, T. J. *Photochem. Photobiol.*, B **2002**, 67, 39.

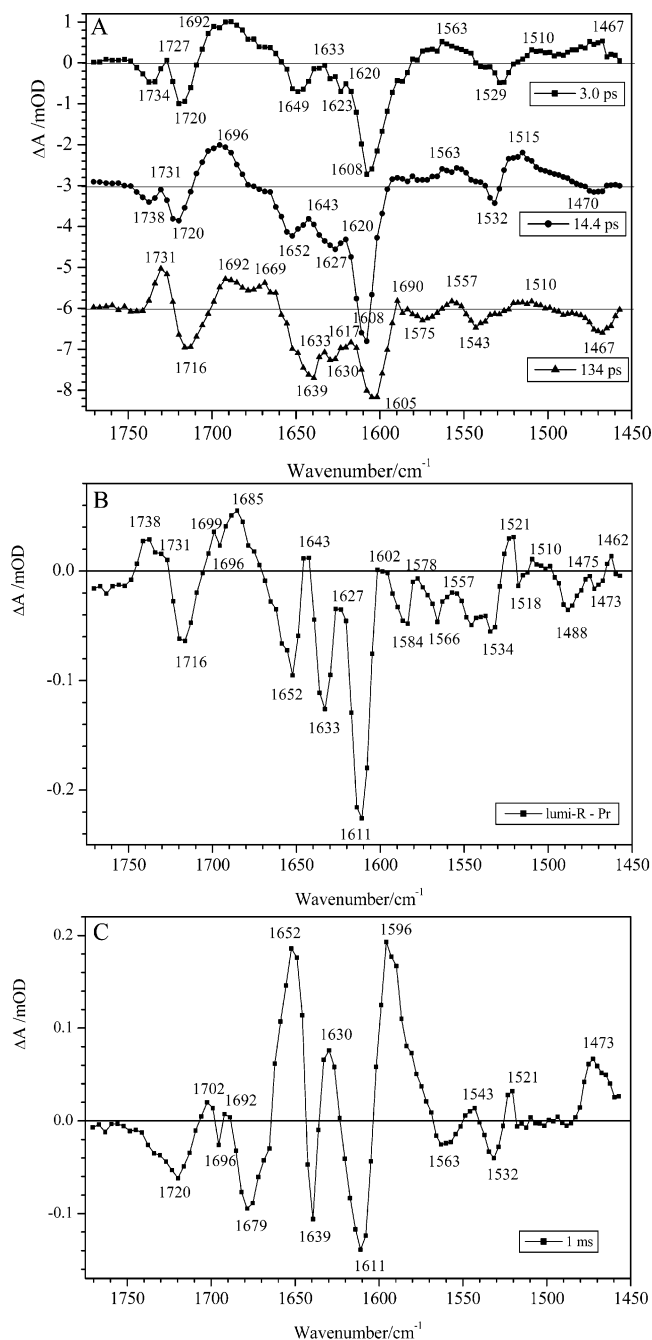


Figure 3. Globally fitted difference spectra describing the absorption changes between 2 ps and 2 ns. (A) Spectra belonging to the three decay components with time constant $\tau_1 = 3$ ps (38%; ■), $\tau_2 = 14$ ps (52%; ●), and $\tau_3 = 134$ ps (10%; ▲). Positive bands belong to S1 and negative bands to Pr in the S0 state. (B) Lumi-R photoproduct minus Pr difference spectrum. (C) Difference spectrum at 1 ms.

at 233 K, whereas Lumi-R of oat phytochrome is formed at 133 K.^{16,17} However, the initial cryo-trapped states from oat phytochrome and Cph1 are both characterized by an upshift of the C₁₉=O mode and may have resulted in accumulation of intermediates further in the photocycle or an entirely different pathway altogether.

In the decay spectra as well as in the Lumi-R minus Pr difference spectrum, the infrared data allow novel identification of three C=C modes. Bleaches are present at 1649, 1623, and 1608 cm⁻¹ at 2 ps after optical excitation, which are assigned to chromophore C=C modes (Figure 1A). The corresponding

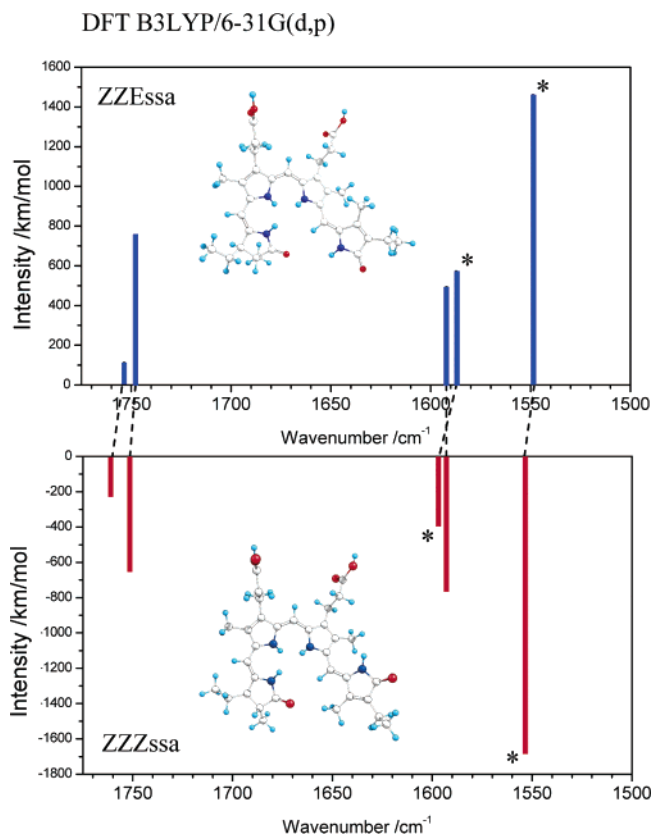
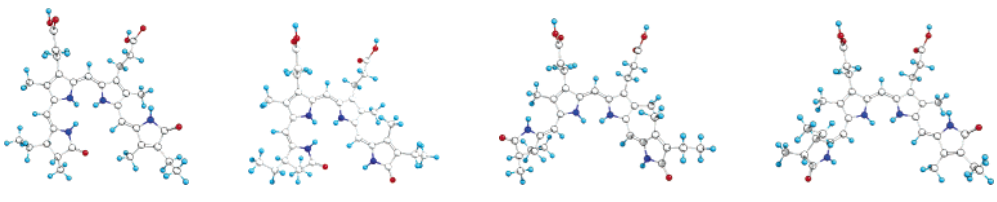


Figure 4. Stick diagram showing scaled frequencies and intensities for infrared active C=O and C=C modes from normal mode calculations at the DFT B3LYP/6-31G(d,p) level. ZZZssa modes are represented as negative, ground-state values, and ZZEssa modes as positive values, reflecting the dipole derivative strengths calculated. Isomerization markers C₁₅=C₁₆ and the delocalized C=C mode are indicated with *.

modes in S1 are expected to be downshifted as a result of reduction of bond orders and have reduced cross sections (Figures 1A and 3A). These three modes are also identified at similar frequencies in the Lumi-R minus Pr difference spectrum (Figure 3B) and thus show the vibrational response of the chromophore C=C modes in the ground-state product Lumi-R after phototransformation of the Pr state. All three modes are interpreted to be downshifted in the Lumi-R state as well, on the basis of the positions of peaks and troughs compared to the generally downshifted decay spectra (Figure 3A,B).

An additional consideration is the observation of two resonance Raman bands in this region in oat phytochrome (1635, 1633, and 1621 cm⁻¹ and 1621, 1582, and 1591 cm⁻¹ for Pr, cryo-trapped Lumi-R, and Pfr in D₂O) and in Cph1 (1629 and 1606 cm⁻¹ and 1634 and 1638 cm⁻¹ in Pr and Pfr in H₂O).^{16,17} A contribution from amide I infrared absorption at 1649 cm⁻¹ in Pfr¹⁸ is observed to grow in at 1652 cm⁻¹ at 1 ms (Figure 3C). However, in the Lumi-R minus Pr difference spectrum (Figure 3B) there is a minimum at 1652 cm⁻¹, which thus belongs to Pr and is assigned to a high-frequency C=C mode: Intense bands in this region belonging to localized C=C modes are observed in tetrapyrrole model compounds such as biliverdin IX and are specific for the cation at low pH (not shown). In addition to the resonance Raman spectroscopy observations in this region, further support for the assignment is the observation

Table 1. Experimental and Calculated Frequencies for Infrared Absorption of C=O and C=C Modes in the Phycocyanobilin Chromophore of Cyanobacterial Phytochrome Cph1^a


	Pr(-)/Lumi-R(+) experimental ν/cm^{-1}	ZZZssa (Pr) DFT normal modes ν/cm^{-1} (int/km/mol)	ZZEssa DFT normal modes ν/cm^{-1} (int/km/mol)	ZZEasa DFT normal modes ν/cm^{-1} (int/km/mol)	EZZasa DFT normal modes ν/cm^{-1} (int/km/mol)
C ₁ =O	1735/1738	1761 (215)	1753 (109)	1788 (449)	1786 (508)
C ₁₉ =O	1716/1685	1752 (643)	1748 (748)	1752 (669)	1753 (639)
C ₁₅ =C ₁₆	1652/1643	1597 (384)	1587 (571)	1594 (325)	1602 (279)
C ₄ =C ₅	1633/1627	1593 (760)	1592 (491)	1598 (486)	1594 (528)
C ₄ =C ₅ ,	1611/1602	1554 (1671)	1548 (1457)	1569 (3604)	1568 (3638)
C ₉ =C ₁₀ ,					
C ₁₀ =C ₁₁ ,					
C ₁₅ =C ₁₆					

^a Experimental infrared absorption frequencies for Pr and Lumi-R photoproduct and frequencies of infrared active normal modes for ZZZssa, ZZEssa, ZZEasa, and EZZasa conformations were calculated at the DFT B3LYP/6-31G(d,p) level, which has been scaled by 0.961.²⁷ Calculated infrared intensities are given in km/mol. See Figure S1 for normal mode representations of the ZZZssa conformation.

of high-frequency C=C modes in olefins.²⁵ The positive charge on protonated tetrapyrroles and extensive conjugation causes the charge alterations in the C=C vibrations that render them IR-active,¹⁵ which is also supported by FTIR ground state and by ultrafast infrared measurements of the biliverdin IX cation (not shown). Normal mode and infrared intensity calculations of the deuterated phycocyanobilin chromophore in the ZZZssa conformation predict three infrared active modes in this region, as experimentally observed, listed with their main contribution in Table 1. The highest frequency C=C normal mode is predicted to be localized and has a main contribution from C₁₅=C₁₆ stretching (Figure 4; S1; Table 1). Consequently, the 1652(-)/1643(+) cm⁻¹ and 1633(-)/1627(+) cm⁻¹ features are proposed to belong to the localized C₁₅=C₁₆ and C₄=C₅ modes, respectively, but in the absence of data collected on specific isotopically labelled material these assignments could conceivably be reversed as the normal mode calculations predict them to be close together (Figure 4; Table 1). However, the discussion focuses on the main observation that both the C₁₅=C₁₆ and the C₄=C₅ modes are downshifted.

The ~1649(-)/1633(+) cm⁻¹ and 1652(-)/1643(+) cm⁻¹ features in the decay spectra and the Lumi-R minus Pr difference spectrum are thus assigned to the C₁₅=C₁₆ mode. Normal mode calculation of the ZZEssa geometry predicts downshifts relative to the ZZZssa isomer of the modes belonging to C₁₅=C₁₆ and also of C₁₉=O (Table 1; Figure 4), both of which are observed in the experimental spectrum and can be taken as additional evidence for C₁₅ Z/E photoisomerization as the primary photochemical event. The observed downshift of C₁₉=O mode in Lumi-R is strong and may indicate increased H-bonding interaction after phototransformation. A downshifting of the C₁=O mode that is also calculated in the ZZEssa geometry is, however, not directly evident. The lowest-frequency C=C mode, observed at 1611(-)/1602(+) cm⁻¹ in the Lumi-R minus Pr difference spectrum, has the highest cross section calculated

and is delocalized with contributions from C₉=C₁₀, C₁₀=C₁₁, C₄=C₅, and C₁₅=C₁₆ (Table 1; Figure S1). This assignment is also in agreement with the shifts observed in Pfr minus Pr static FTIR difference spectrum in this region with ¹³C labeling of methine bridge carbons in the chromophore.¹⁸ C₁₅ Z/E photoisomerization is predictably calculated to downshift this mode as well (Table 1; Figure 4).

However, the mode at 1632 cm⁻¹, assigned to C₄=C₅ localized vibration, is equally downshifted in the Lumi-R minus Pr difference spectrum (Figure 3B), which is not predicted to result from isomerization at C₁₅ (Figure 4; Table 1) and thus indicates changes near C₅. For completeness, normal mode calculations were performed and are also reported in the optimized ZZEasa and EZZasa geometries, neither of which would be predicted to downshift the C₄=C₅ mode (Table 1). Since normal mode calculations are only meaningful for energy-minimized geometries, these cannot take into account partial low order bond rotations unless redundant coordinates are included. For example, partial rotation around the C₅-C₆ bond has been discussed in reaction models on the basis of NMR and optical characteristics⁶ and resonance Raman spectroscopy measurements.¹⁴ Rotation of the C₅-C₆ bond toward its *syn*-minimized configuration would decrease the C₄=C₅ local bond order and would thus lead to a downshift of the mode assigned to this bond, at 1633 and 1627 cm⁻¹ in Pr and Lumi-R, respectively. TDDFT calculations have shown that such a bond rotation would be associated with red-shifted visible absorption.⁶ Small rotations of the C₅-C₆ bond are predicted not to affect the bond orders at C₉=C₁₀, C₁₀=C₁₁, and C₁₅=C₁₆ significantly, as measured via their geometry-optimized bond lengths, and thus the effect could be relatively localized.

Further indications of the additional changes in Lumi-R are the reduced cross sections of the three C=C modes (Figure 3B) and the only slightly red-shifted visible absorption.¹² Mechanisms that could explain the reduced infrared intensities in Lumi-R are stable charge changes or changes in symmetry or possibly changes in conjugation. It is noted that the increase in

(25) Gunzler, H.; Gremlich, H.-U. *IR Spectroscopy: An Introduction*; Wiley-VCH: Weinheim, Germany, 2002; p 187.

infrared cross section of the C=C modes between 100 ps (Lumi-R, Figure 3B) and 1 ms (Figure 3C) and the further gain in Pfr¹⁸ of C=C modes also correspond with red-shifted visible absorption that is developed on these timescales.^{7,8} The infrared observations could therefore be explained by models that considered C₅-C₆ bond angle changes in the reaction pathway.^{6,14}

In conclusion, the time-resolved measurement of the mid-infrared absorption of the initial Lumi-R photoproduct has provided evidence for changes at C₁₅ as well as at C₅, from the novel observation of chromophore C=C modes on an ultrafast timescale. We note that, although previous Raman mode assignment assumed a ZZZasa conformation in the Pr state, which predicted the Raman active C₄=C₅ mode at higher frequency than the C₁₅=C₁₆ mode,^{13,14,26} from our infrared data we also assign the Pr mode at $\sim 1635\text{ cm}^{-1}$ in D₂O to C₄=C₅

stretching. The spectral changes in Lumi-R can be interpreted with C₁₅ Z/E photoisomerization in addition to changes near C₅, which could be low bond order torsional angle changes of the C₅-C₆ bond.

Acknowledgment. J.J.v.T. is a Royal Society University Research Fellow. We thank Peter Rich for helpful discussion and Jenny Gibson for technical assistance. We acknowledge access to the PIRATE ultrafast infrared spectroscopy facility at the Rutherford Appleton Laboratory, through applications US/19/B/2/05 and US/20/B/1/06.

Supporting Information Available: Normal mode representations in the ZZZssa conformation. Complete ref 23. This material is available free of charge via the Internet at <http://pubs.acs.org>.

JA0660709

(26) Borucki, B.; von Stetten, D.; Seibeck, S.; Lamparter, T.; Michael, N.; Mroginski, M. A.; Otto, H.; Murgida, D. H.; Heyn, M. P.; Hildebrandt, P. *J. Biol. Chem.* **2005**, *280*, 34358.

(27) Irikura, K. K.; Johnson, R. D. I.; Nacker, R. N. *J. Phys. Chem. A* **2005**, *109*, 8430.